Proceedings of the ASME 2018 37th International Conference on Ocean, Offshore and Arctic Engineering
OMAE2018
June 17-22, 2018, Madrid, Spain

OMAE2018-77169

DESIGN OF A TIDAL TURBINE ARRAY FOR THE BOHAI STRAIT, CHINA

Lei Chen
Department of Engineering Science
University of Oxford
Oxford OX1 3PJ
United Kingdom
lei.chen@eng.ox.ac.uk

Paul A. J. Bonar
School of Engineering
University of Edinburgh
Edinburgh EH9 3FB
United Kingdom
p.bonar@ed.ac.uk

Thomas A. A. Adcock
Department of Engineering Science
University of Oxford
Oxford OX1 3PJ
United Kingdom
thomas.adcock@eng.ox.ac.uk

ABSTRACT

In this paper, we consider array design strategies to maximise the power available to turbines placed in the Bohai Strait, which is considered to be one of China's most promising candidate sites for tidal stream power. The discontinuous Galerkin version of the open-source hydrodynamic model ADCIRC is used to simulate flow through the strait and tidal turbines are introduced using a sub-grid scale actuator disc model. New design algorithms based on key theoretical results are used to build large arrays, which are then compared in terms of both the collective power output and the power produced per turbine. The results of the analysis are used to draw general conclusions about the optimal design of tidal turbine arrays.

1 INTRODUCTION

The development of tidal stream power is at an early stage. A number of prototype devices have been tested in isolation and the world's first large-scale tidal turbine array is presently being installed in Scotland's Pentland Firth. However, it is still unclear how a large number of tidal stream turbines should be arranged to maximise their collective power output. This optimal arrangement problem is complicated by the fact that tidal turbines interact with the flow as they apply the force necessary to do work and generate power. These interactions take place across a wide range of length scales — from the scale of the turbine blade to the scale of the ocean basin (see Figure 5 in Adcock et al. [1], for instance) — which makes the modelling and optimisation of large turbine arrays a formidable challenge.

Researchers have explored this optimal arrangement problem using two main approaches. The first of these, which was pioneered by a group at Imperial College London [e.g. 2; 3], uses gradient-based optimisation methods to design tidal turbine arrays. This approach is promising but computationally intensive, and makes it difficult to account properly for turbine characteristics and inter-turbine interactions. The second involves greatly simplifying the problem so that analytical or idealised numerical methods may be applied. Garrett & Cummins [4] used this approach to represent a turbine array as a simple resistive force, and to demonstrate that there is a maximum amount of power that may be extracted from a tidal channel. Vennell [5] later replaced this resistive force with an actuator disc model to represent an array of turbines spanning the channel width. His analysis suggests that array performance is maximised by arranging the turbines in a single cross-stream row (to maximise their global blockage), and demonstrates a diminishing return in power on the addition of new rows downstream [see also 6; 7]. Vennell showed that optimum performance requires turbines to be 'tuned' for a given channel, and later extended this work to include time-variable resistances and turbine tunings [8; 9]. Nishino & Willden [10] then considered a different problem, that of a steady flow partially blocked by an array of turbines. Their analysis suggests that array performance is not maximised by distributing the turbines evenly across the cross-section, but rather by clustering them closer together to exploit constructive local blockage effects. Forthcoming work by the authors and other colleagues has extended this analysis to describe the effects of local blockage in oscillatory flow.

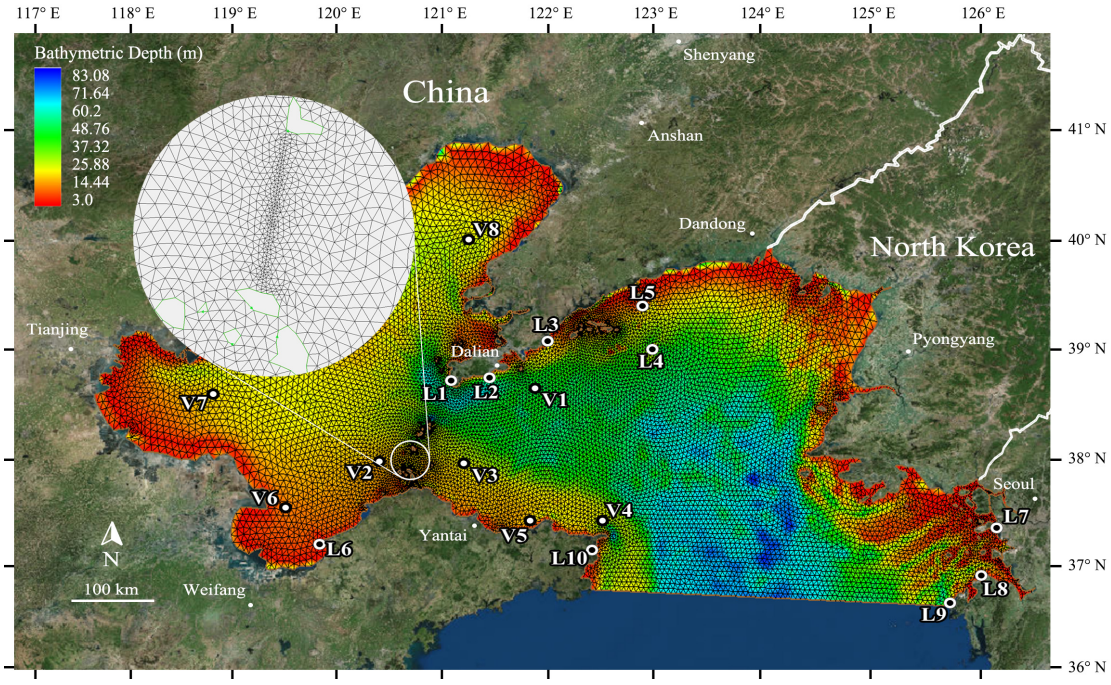

FIGURE 1. Bohai Sea model domain and numerical mesh with contours of bathymetric depth and field measurement markers.

In this paper, we develop new array design algorithms, based on these key theoretical results, to maximise the power available to turbines placed in a narrow tidal strait. We use these algorithms to design turbine arrays for the Bohai Strait, which is considered to be one of China's most promising candidate sites for tidal stream power. Real sites such as this are of course unique but we nonetheless aim to draw general conclusions to better inform the design of tidal turbine arrays.

The paper is structured as follows. We describe the models used to capture the natural hydrodynamics of a real site and introduce idealised representations of tidal turbines in §2. We then discuss the development of the Bohai Strait model and its validation against field measurements. In §3, we introduce the different algorithms used to build the turbine arrays and analyse how these perform in the Bohai Strait. Finally, we discuss possible extensions to this work before concluding with §4.

2 MODEL

Numerical scheme

The discontinuous Galerkin (DG) version of the open-source hydrodynamic model ADCIRC [11; 12] is used to simulate flow through China's Bohai Strait. This code solves the depth-averaged shallow water equations, which assume that the velocity profile is uniform over the depth. The equations are solved in a locally conservative form, which allows an actuator disc model to be placed between adjacent elements in the numerical mesh [13–15]. For this study, we use the open channel actuator disc model derived by Houlsby et al. [13], which is a finite Froude number extension of the volume flux-constrained actuator disc model of Garrett & Cummins [16].

Following Houlsby et al. [13], the turbines are defined by a local blockage ratio B and a local wake velocity coefficient α_4. Flow passing through the turbines experiences a momentum sink as power is extracted. This momentum sink is represented as a discontinuous change in fluid depth $\triangle h$, given by:

$$\frac{1}{2}\left(\frac{\triangle h}{h}\right)^3 - \frac{3}{2}\left(\frac{\triangle h}{h}\right)^2 + \left(1 - Fr^2 + \frac{C_T B Fr^2}{2}\right)\left(\frac{\triangle h}{h}\right) - \frac{C_T B Fr^2}{2} = 0, \quad (1)$$

in which $Fr = u/gh$ is the local Froude number, with h the local depth and u the streamwise component of depth-averaged velocity, ρ is the fluid density, and C_T is the local thrust coefficient. The extractable power is then given by:

$$P_{ex} = \rho g u b h \triangle h \left(1 - Fr^2 \frac{(1 - \triangle h/(2h))}{(1 - \triangle h/h)^2}\right), \quad (2)$$

in which b is the width of the local flow passage and g is acceleration due to gravity. The available power is the amount remaining when the power lost in local wake mixing is subtracted from the extractable power, and is given to good

approximation by:

$$P = \alpha_2 \left(1 - \frac{1}{2}\frac{\triangle h}{h}\right) P_{ex}, \tag{3}$$

in which α_2 is the ratio of turbine throughflow velocity to upstream velocity.

Adopting this model of energy extraction requires a number of simplifying assumptions, but the sub-grid scale model has nonetheless been shown to agree well with laboratory-scale physical experiments [17]. Here we assume that the device-scale mixing length is sufficiently small (compared to the size of mesh elements) as to be described as a sub-grid scale process, and that the flow through the turbines varies sufficiently slowly as to be considered quasi-steady. The power available to the actuator disc is considered an upper bound on the power available to a real turbine, which would experience additional losses due to sheared inflow, viscous drag, mechanical and electrical losses, etc.

Model details

The model is built to simulate the tidal hydrodynamics of the Bohai Strait, which connects the Bohai Sea (a semi-enclosed body of water) to the Yellow Sea and is considered to be one of China's most promising candidate sites for tidal stream power. As shown in Figure 1, the model domain covers the entire Bohai area. Aquaveo's Surface Water Modelling System (SMS) is used to generate an unstructured mesh comprising 12,618 nodes and 23,885 elements with lengths varying from 1.5 km down to 300 m at the location of interest. Bathymetry data are obtained from GEBCO's 30 arc-second global grid at a spatial resolution of ∼950 m. A wetting and drying function is used because the Bohai Sea is relatively shallow [18]. To ease computation and improve model stability, a number of small islands and channels have been removed.

The southern ocean boundary is forced with tidal constituents from the Le Provost database [19] and placed sufficiently far from the area of interest as to be unaffected by the changes introduced by the turbines. A grid convergence study is then performed to confirm that the model results are mesh and time step independent. The relevant literature suggests that the Bohai Sea has four principal tidal constituents — that is to say, in this region the tide-generating force due to the gravitational pull of the Sun and Moon comprises four principal components — the diurnal K1 and O1 tides and the semidiurnal M2 and S2 tides [20]. The Le Provost database is used to relate these force components to displacements of the ocean boundary. However, because predictions from the global tidal model can be inaccurate in some locations, validation tests must be performed. Comparing the results obtained using the initial tidal forcing with other models of the area [21] reveals poor agreement at the eastern side of the ocean boundary. This may be due to the present model's failure to capture the effect of the Coriolis force pushing tides towards the Korean Peninsula and increasing their amplitude. A larger numerical model, covering the Bohai, Yellow, and East China Seas, is then built in order to obtain more accurate boundary conditions for the smaller Bohai Sea model.

Model validation

The model is validated by using harmonic analysis to compare the water levels and current velocities predicted by the numerical model with those predicted by the TotalTide, a software package used by the British Admiralty to predict sea levels and currents. It uses field measurements of water levels and current velocities to make harmonic predictions, which can be used to validate a numerical model in the absence of site-specific data. The simulation period commences on the first day of 2016. The tidal forcing is ramped up over a period of 4 days, and the model is then allowed to run for another 1 day before results from the following 14 days are extracted for harmonic analysis. Model predictions are also found to give good visual agreement with cotidal charts published in earlier works [e.g. 22].

The water level amplitudes and phases predicted by the numerical model are compared with the predictions from TotalTide at the ten water level measurement stations (L1–L10) shown in Figure 1. The predictions for M2 and K1 tides are compared in Tables 1 and 2. Agreement between the predictions is fair, with amplitude errors generally less than 15% and phase errors generally less than 20^o. Some discrepancy is to be expected because these points are located within the inter-tidal zone, where the water is shallow and sensitive to factors such as seabed drag and wetting and drying — all of which present modelling challenges. Nonetheless, the results indicate that the present model is capable of capturing the key features of the tidal elevations.

Current velocities are calibrated by adjusting the seabed drag coefficient to match the model results to the TotalTide predictions. The drag on the flow due to bed roughness is given by $F = \rho A \mathbf{u}|\mathbf{u}|C_d$, in which ρ is the density of seawater, A is the area of the seabed, $\mathbf{u}$ is the depth-averaged velocity vector, and C_d is the dimensionless seabed drag coefficient. Calibration of depth-averaged velocities is difficult because current speeds vary considerably with position and within the water column. For the Bohai Sea, there are limited current velocity measurements and those that are available tend to be of poor quality. For this shallow domain, a hybrid nonlinear bottom friction law is applied. A C_d value of 0.001 — set to increase slowly (by a factor of $[1+(10/d)^{10}]^{(1/30)}$) in depths $d < 10$ m in order to maintain model stability — is found to provide the best fit between the current velocities predicted by the numerical model and those predicted by TotalTide. This agrees well with other studies of the Bohai Sea, which show the region to have relatively low bed roughness [23]. Table 3 compares the predicted current velocities at the seven current measurement stations (V1–V7) shown in Figure 1. The quality of the TotalTide measurements are unknown so some

TABLE 1. Predicted water level amplitudes (m).

	M2 tide			K1 tide		
Station	TotalTide	ADCIRC	error (%)	TotalTide	ADCIRC	error (%)
L1	0.61	0.54	-11.48	0.13	0.21	+61.54
L2	0.89	0.79	-11.24	0.23	0.26	+13.04
L3	1.15	1.06	-7.83	0.29	0.34	+17.24
L4	1.27	1.17	-7.87	0.37	0.36	-2.70
L5	1.58	1.56	-1.27	0.35	0.41	+17.14
L6	0.50	0.50	+0.00	0.20	0.24	+20.00
L7	2.87	3.20	+11.50	0.46	0.32	-30.44
L8	2.62	2.91	+11.07	0.40	0.33	-17.50
L9	2.20	2.15	-2.27	0.37	0.31	-16.22
L10	0.50	0.51	+2.00	0.30	0.25	-16.67

TABLE 2. Relative phases of water level signals (degrees).

	M2 tide			K1 tide		
Station	TotalTide	ADCIRC	error (^{o})	TotalTide	ADCIRC	error (^{o})
L1–L2	-27	-29	-2	-36	-34	+2
L2–L3	-18	-20	-2	+342	-15	-357
L3–L4	-22	-28	-6	-16	-14	+2
L4–L5	+3	+8	+5	+10	+4	-6
L5–L6	+14	+128	+114	-139	-133	+6
L6–L7	-132	92	+224	+74	+66	-8
L7–L8	-12	-22	-10	+6	-21	-27
L8–L9	-14	-20	-6	-14	+6	+20
L9–L10	-96	-54	+42	-2	-19	-17
L10–L1	+304	-56	-360	-7	-16	-9

TABLE 3. Major axis amplitudes (m) and relative phases (degrees) of depth-averaged velocity signals.

	Amplitudes				Phase		
Station	TotalTide	ADCIRC	error (%)	Station	TotalTide	ADCIRC	error (^{o})
V1	0.22	0.34	+54.54	V1–V2	92	132	+40
V2	0.18	0.22	+22.22	V2–V3	20	-20	-40
V3	0.65	0.80	+23.10	V3–V4	-113	-125	-12
V4	0.28	0.15	-46.43	V4–V5	78	55	-23
V5	0.25	0.52	+108.00	V5–V6	74	108	+34
V6	0.38	0.50	+31.58	V6–V7	-116	-128	-12
V7	0.41	0.51	+24.39	V7–V1	-35	-22	+13

discrepancies are to be expected. Overall, however, the model is found to capture the basic physics of the Bohai Sea reasonably well. Anecdotal evidence from other researchers suggests that modelling this region is more difficult than most — this was certainly our experience.

Sources of error

Here we have two principal sources of error: the quality of the input data and the simplifying assumptions that have been made in building the model, and the quality of the data used for validation. The accuracy of the model is highly dependent on the accuracy of the bathymetry data, especially in the shallow regions. The resolution of the GEBCO data is insufficient to capture the small, localised tidal dynamics along the complex coastlines and close to the islands where those observation stations are typically located. The Le Provost database, which is derived from older, empirical data, may contain inaccuracies and the code may struggle to correctly interpolate tidal frequencies and amplitudes close to the ocean boundary. The model has also been simplified by smoothing the coastlines, such that it does not fully account for small structures such as bays and estuaries. Another key limitation is the inability of the depth-averaged model to capture the more complicated flows around islands and headlands, where the 3D effects can no longer be neglected [24].

The TotalTide data is also likely imperfect. However, water level data are generally considered more reliable than the current measurements, as it is supported by data sourced from other papers [21]. Additionally, the Bohai Sea's coastal zone has witnessed a large amount of economic development in the last ten years, resulting in a significant amount of coastal reclamation work to meet the demands of the increased urbanisation and industrialisation. What was previously wetland and tidal flats on the land closest to the seafront has been developed with features such as seawalls and harbours [25]. This means that the TotalTide data may no longer accurately reflect the movements of water in the region.

Turbine implementation

The numerical mesh is then modified to place rows of tidal turbines in the Bohai Strait, which is located between China's North Changshan island and Tuoji Island (Figure 2). The distance between these islands is $\sim$20 km and the average water depth is $\sim$25 m, so the turbines have been designed with a diameter of 10 m. To avoid having to adjust the mesh each time a new row is added, the code is modified to allow multiple rows of turbines to be placed within the edge between adjacent mesh elements. To facilitate this modification, it is assumed that each new row within a given edge is placed directly behind the previous row(s), and that each row within a given edge experiences the same flow conditions: identical upstream velocity, water depth, and Froude number. This assumption is not entirely unrealistic because many practical situations will require tidal turbines to be closely spaced in the streamwise direction. The wake mixing length of a tidal turbine is typically 20 times the diameter [26], however, which is larger than the $\sim$300 m mesh resolution. This discrepancy may result in minor differences in the power calculations, but these are neglected because the available power is determined mainly by turbine thrust and not turbulent mixing. Time-variable tuning strategies will be explored in a future work but, in this study, the wake velocity coefficients are held constant throughout the tidal cycle.

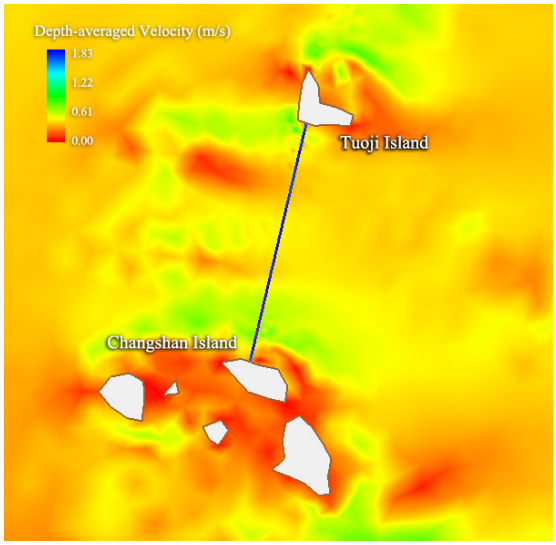

FIGURE 2. Contours of unexploited depth-averaged velocity through the Bohai Strait. The black line marks the proposed location for the turbine array.

3 Array design

Strategies

The naturally occurring kinetic energy flux can be a useful metric in assessing the tidal stream resource. The natural kinetic energy flux formed the basis of early resource assessments [e.g. 27], which multiplied its value by some arbitrary number (less than one) to give an estimate of the resource [28]. This approach has since been shown to be flawed because the natural kinetic energy flux is not directly related to the maximum extractable power [e.g. 29], but it is clearly a useful starting point for resource assessment and the optimal arrangement of tidal turbines. We use this metric as the basis of our new array design strategies.

The three design strategies trialled in this paper are illustrated in Figures 3, 4, and 5. The cross-section is divided into 50 sections of equal width and the sections with a mean water depth of less than 1.5 turbine diameters are excluded from the analysis. Arrays are then built incrementally by placing turbines in the section of highest kinetic energy flux (averaged over the tidal cycle), and filling each section up to a blockage ratio of 0.4 before moving onto a new section, chosen by one of three design strategies. The first strategy is based purely on the natural kinetic flux and does not account for feedback between the turbines and the flow. The second and third strategies do account for feedback effects; the former requires all the turbines to be placed in a single cross-stream row, while the latter allows the turbines to be deployed in multiple rows (though within a single turbine edge).

The first strategy, which does not account for feedback between the turbines and the flow, requires the model to be run only once but the second and third require many numerical simula-

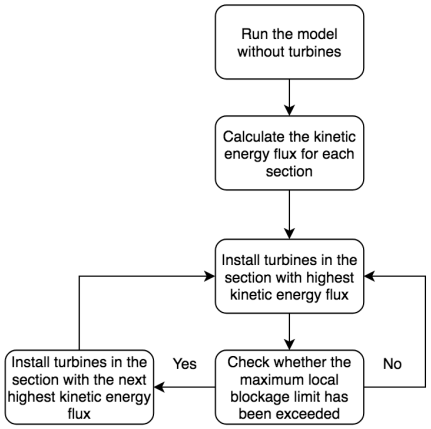

FIGURE 3. Array design algorithm for strategy 1

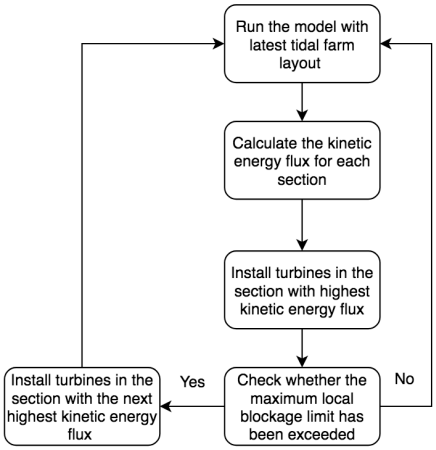

FIGURE 4. Array design algorithm for strategy 2

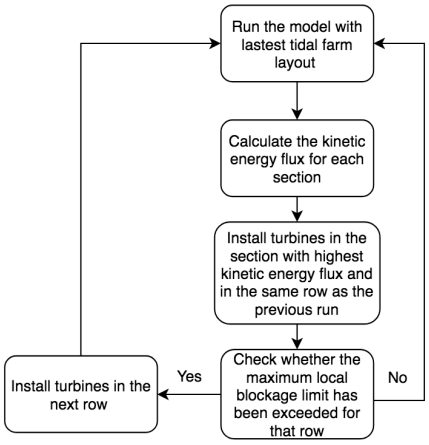

FIGURE 5. Array design algorithm for strategy 3

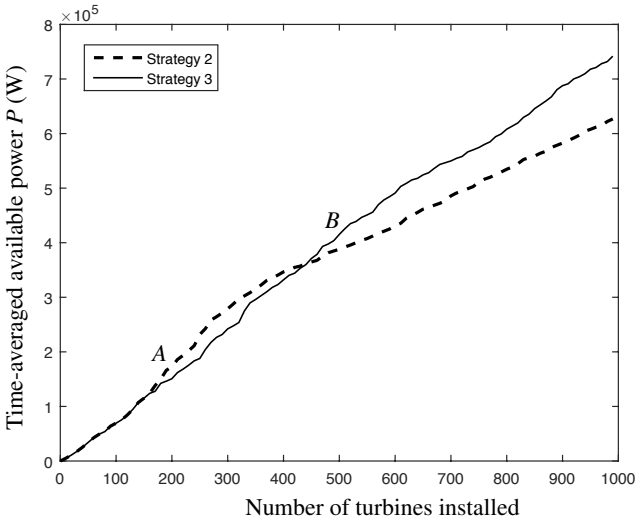

FIGURE 6. Variation in time-averaged available power P with number of turbines installed.

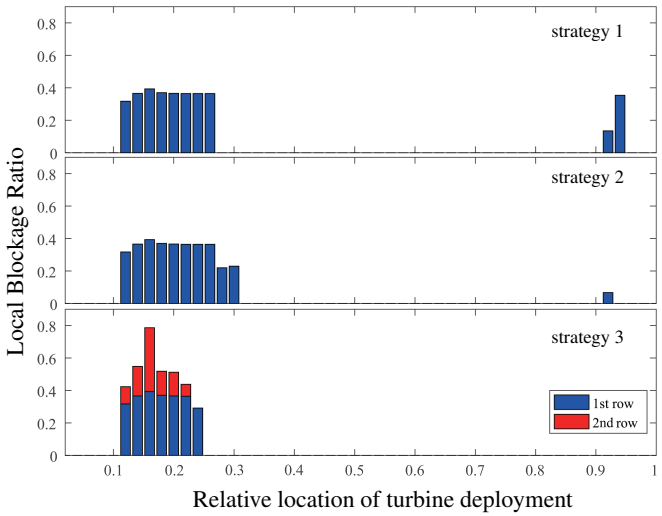

FIGURE 7. Optimal arrangements (cross-sectional views of local blockage distributions) of 440 turbines corresponding to the different development strategies.

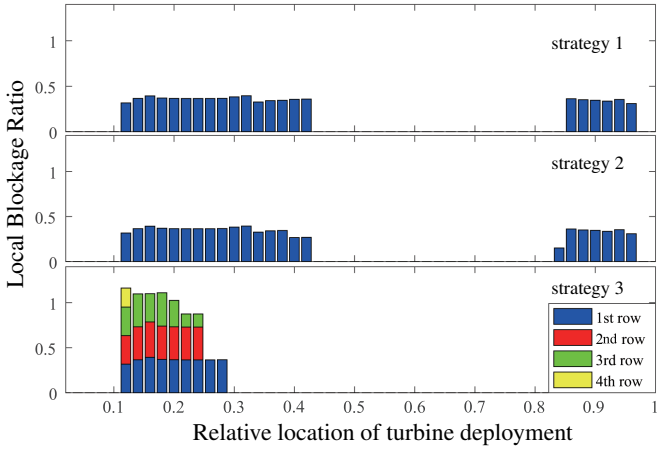

FIGURE 8. Optimal arrangements (cross-sectional views of local blockage distributions) of 1000 turbines corresponding to the different development strategies.

tions. For this study, 1000 turbines are to be installed in groups of 10. To facilitate the large number of simulations required, the problem is simplified: the model is allowed to spin up for 1 day before results from the following 3 days are extracted and time-averaged; the wake velocity coefficient is held constant as the arrays are built; and flow is driven by a single tidal constituent: the M2. The use of a single constituent is expected to make only a small difference to the dynamic balance and thus the optimal turbine layout. It is also worth noting that the adjoint approach [e.g. 2; 3] typically simplifies the problem further to consider only steady flow. However, this neglects the effects of flow reversal, which forthcoming work by the authors has shown to be significant, not necessarily for the channel considered here but certainly for inertial channels.

Analysis

Figure 6 presents a comparison of the time-averaged power available to the arrays built using strategies 2 and 3. The power output is shown to increase monotonically with the number of turbines installed, and the curves for the two strategies are shown to match exactly up to point A, because for both strategies the first 170 turbines are installed in a single cross-stream row. Beyond this point, however, the outputs diverge as strategy 2 continues to add turbines to the same row whereas strategy 3 begins placing turbines in a second row behind the first. Between points A (170 turbines installed) and B (440 turbines installed), strategy 2 produces more power than strategy 3, which is somewhat counterintuitive, given that it is the more constrained strategy. Beyond point B, however, strategy 3 begins to outperform strategy 2. The arrays produced by the different strategies for 440 and 1000 turbines are illustrated in figures 7 and 8.

The difference in power produced by the two strategies is explained as the choice between placing turbines only in parallel (strategy 2) or also allowing placement of turbines in series (strategy 3) [30]. The optimal arrangement is of course highly dependent on the site geometry and flow dynamics. Adding turbines in parallel increases their global blockage, thereby increasing the available power, whereas adding turbines in series allows for much greater thrust to be applied to the flow. The series configuration is more effective in cases where the kinetic energy flux is higher in certain sections. The initial benefit from the parallel arrangement, between points A and B and due to the global blockage effect, is eventually exceeded by the benefit from the

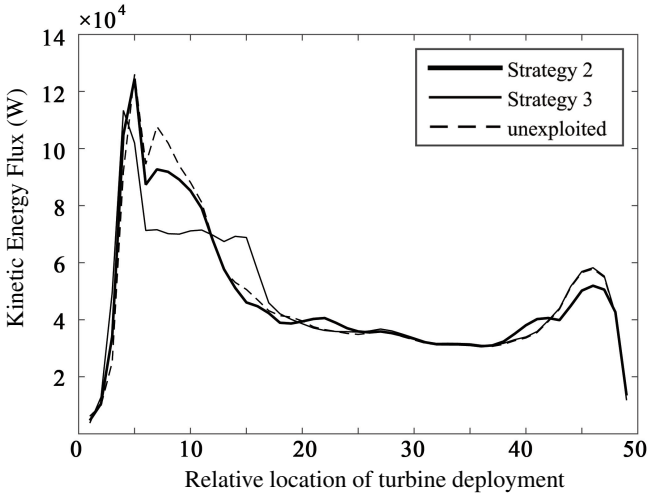

FIGURE 9. Spanwise kinetic energy flux profile for the unexploited case and for arrays of 1000 turbines built using strategies 2 and 3.

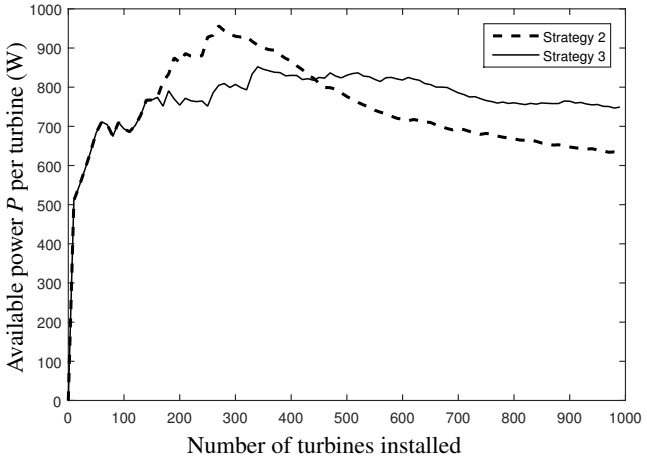

FIGURE 10. Variation in power per turbine with number of turbines installed.

series arrangement, which allows several rows of turbines to be placed at the section with the higher kinetic flux. For a certain number of turbines strategy 2 is better, but strategy 3 will prove more beneficial overall.

Figure 9 plots the spanwise kinetic energy flux profile before and after the installation of the turbine array, and shows two peaks at the ends of the profile, with a left peak much higher than the right. In strategy 2, the turbines are constrained to be placed within a single row, so the left peak is exploited first, before the next deployment is made to exploit the right peak. The placement of turbines is less constrained in strategy 3, which allows for the installation of turbines in the highest kinetic flux sections. The multiple rows installed in strategy 3 make the largest changes to the kinetic energy flux profile, reducing the flow through the array and enhancing the array-scale bypass flow. The disadvantage

TABLE 4. Time-averaged power available (W) to different array design strategies.

Number of turbines	Even	1	2	3
440	2.88 x 10^5	7.86 x 10^5	8.13 x 10^5	7.74 x 10^5
1000	8.29 x 10^5	1.44 x 10^6	1.42 x 10^6	1.51 x 10^6

of strategy 2, as compared to strategy 3, is that turbines must be placed in the lower kinetic energy flux sections much sooner.

Figure 10 shows the growth of mean power per turbine for strategies 2 and 3. The global blockage effect initially increases not only the combined power output but also the power per turbine. The power per turbine then starts to decline, however, as each new turbine is placed in a less favourable location. It is surprising that the curve for strategy 3 remains relatively flat even after three rows are installed, since the power is proportional to the cube of velocity and the thrust from three rows should significantly reduce the rate of flow through the array. This suggests that there is no obvious diminishing return on the placement of successive turbine rows in this case. To explain this, we make some simplifying assumptions about the hydrodynamics of the site and compare it to the idealised channel model of Garrett & Cummins [4]. The phase lag between head difference and current at the site is found to be $\sim 30^o$, which corresponds to a natural dynamic balance λ_0 of ~ 2. This implies that the natural impedance of the site is quite high, giving it characteristics similar to a drag-dominated site. This explains why the kinetic energy flux profile appears to be relatively insensitive to the thrust from turbines, allowing multiple rows to be installed in the 'left peak' area.

Additional tidal constituents

Having explored optimal arrangements for turbines in a simplified flow through the Bohai Strait, a more realistic situation is now considered. In this scenario, the model is forced with both M2 and K1 tides and allowed to spin up for 4 days from still water conditions before results from the following 15 days are recorded for analysis. The additional tidal constituents and longer simulation period are found to increase the available power by $\sim 100\%$. Optimal wake velocity coefficients are sought to calculate the maximum available power, although given the 'drag-dominated' nature of the site these were found to be close to $\alpha_4 = 1/3$ [see 5]. A fourth array design strategy, in which the turbines are distributed evenly across the site (i.e. turbines in each section but with variable local blockage), is included for comparison. Table 4 shows the results obtained for deployments of 440 and 1000 turbines using the four different strategies (including the 'even' strategy) for the case involving the additional tidal constituent and longer model run time.

For a deployment of 440 turbines strategy 2 is shown to produce more power, but for 1000 turbines strategy 3 proves more beneficial. However, it is difficult to distinguish here between the

effects of the kinetic energy flux profile and the effects of global and local blockage. These three effects will have contributed in different ways to the different strategies, but it is difficult to separate these effects at a real site. This will be explored in greater detail in future work.

Interestingly, in this case strategy 1 (the naturally occurring kinetic energy flux approach) produces an optimal array very similar to that produced by strategy 2. Strategy 1 appears effective in this case but this is likely only due to the 'drag-dominated' nature of the site. It is not recommended that strategy 1 be used more generally. Based on the results above, a general suggestion for tidal farm arrangements can be given, however: depending on the specific site and the proposed number of turbines, arrangement strategies such as those developed here can be used to inform the design of tidal turbine arrays.

4 Conclusions

In this paper, we have explored different strategies for building tidal turbine arrays in China's Bohai Strait. The resource in this region is relatively small and so it is unlikely to make a promising site for a tidal stream power development. This analysis, however, allows us to examine the difficulties of arranging tidal turbines in real locations with varying bathymetry and complex flow patterns. New design strategies based on kinetic energy flux profiles are used to design tidal turbine arrays. The optimal arrangements are found to be highly dependent on both the dynamics of the site and the number of turbines to be installed. For this 'drag-dominated' site, we found it advantageous to concentrate our turbines in the areas of highest kinetic energy flux, but we also note that this may not be the optimal strategy for an 'inertia-dominated' site [see 4].

We have identified several processes which affect the optimal arrangement of tidal turbines at real sites:

• The natural distribution of kinetic energy flux. This is particularly important for small deployments of turbines.

• Flow diversion. Turbines must exert a force on the incoming flow in order to extract power, which results in flow diversion and a reduction in throughflow velocity.

• Local blockage. Increasing the density with which turbines are packed means they can be operated more efficiently — their power coefficient changes.

The optimal arrangement problem remains a complex one. We have considered a few different array design strategies but have also tried to analyse the underlying physics, which is especially difficult for real sites. We recognise that whilst strategies based purely on numerical optimisation have their place, there is potential to improve these with intermediate simpler strategies such as those used here and with insights into the key physics of the problem.

REFERENCES

[1] Adcock, T.A.A., Draper, S., Nishino, T., 2015. "Tidal power generation – A review of hydrodynamic modelling". *P. I. Mech. Eng. A – J. Pow. Energ.* **229**(7): 755–771.

[2] Funke, S.W., Farrell, P.E., Piggott, M.D., 2014. "Tidal turbine array optimisation using the adjoint approach". *Renew. Energ.* **63**: 658–673.

[3] Funke, S.W., Kramer, S.C., Piggott, M.D., 2016. "Design optimisation and resource assessment for tidal-stream renewable energy farms using a new continuous turbine approach". *Renew. Energ.* **99**: 1046–1061.

[4] Garrett, C., Cummins, P., 2005. "The power potential of tidal currents in channels". *Proc. R. Soc. A* **461**(2060): 2563–2572.

[5] Vennell, R., 2010. "Tuning turbines in a tidal channel". *J. Fluid Mech.* **663**: 253–267.

[6] Vennell, R., 2012. "Realizing the potential of tidal currents and the efficiency of turbine farms in a channel". *Renew. Energ.* **47**: 95–102.

[7] Adcock, T.A.A., Draper, S., Houlsby, G.T., Borthwick, A.G.L., Serhadlıoğlu, S., 2013. "The available power from tidal stream turbines in the Pentland Firth". *Proc. R. Soc. A* **469**(2157): 20130072.

[8] Vennell, R., Adcock, T.A.A., 2014. "Energy storage inherent in large tidal turbine farms". *Proc. R. Soc. A* **470**(2166): 20130580.

[9] Vennell, R., 2016. "An optimal tuning strategy for tidal turbines". *Proc. R. Soc. A* **472**(2195): 20160047.

[10] Nishino, T., Willden, R.H.J., 2012. "The efficiency of an array of tidal turbines partially blocking a wide channel". *J. Fluid Mech.* **708**: 596–606.

[11] Kubatko, E.J., Westerink, J.J., Dawson, C., 2006. "hp discontinuous Galerkin methods for advection dominated problems in shallow water flow". *Comput. Meth. Appl. Mech. Eng.* **196**(1-3): 437–451.

[12] Kubatko, E.J., Bunya, S., Dawson, C., Westerink, J.J., 2009. "Dynamic p-adaptive Runge-Kutta discontinuous Galerkin methods for the shallow water equations". *Comp. Meth. Appl. Mech. Eng.* **198**(21-26): 1766–1774.

[13] Houlsby, G.T., Draper, S., Oldfield, M.L.G., 2008. "Application of linear momentum actuator disc theory to open channel flow". Tech. Rep. OUEL 2296/08, Department of Engineering Science, University of Oxford.

[14] Draper, S., Houlsby, G.T., Oldfield, M.L.G., Borthwick, A.G.L., 2010. "Modelling tidal energy extraction in a depth-averaged coastal domain". *IET Renew. Pow. Gener.* **4**(6): 545–554.

[15] Serhadlıoğlu, S., 2014. "Tidal stream resource assessment of the Anglesey Skerries and the Bristol Channel". DPhil Thesis, University of Oxford, UK.

[16] Garrett, C., Cummins, P., 2007. "The efficiency of a turbine in a tidal channel". *J. Fluid Mech.* **588**: 243–251.

[17] Draper, S., Stallard, T., Stansby, P., Way, S., Adcock, T., 2013. Laboratory scale experiments and preliminary modelling to investigate basin scale tidal stream energy extraction. In: *10th European Wave and Tidal Energy Conference, Aalborg, Denmark*.

[18] Yang, H.-Y., Chen, B., Barter, M., Piersma, T., Zhou, C.-F., Li, F.-S., Zhang, Z.-W., 2011. "Impacts of tidal land reclamation in Bohai Bay, China: Ongoing losses of critical Yellow Sea waterbird staging and wintering sites". *Bird Conserv. Int.* **21**(3): 241–259.

[19] Le Provost, C., Genco, M.-L., Lyard, F., 1995. “Modeling and predicting tides over the World Ocean”. *Quant. Skill Assess. Coast. Ocean Models*: 175–201.
[20] Li, Y., Zhang, H., Tang, C., Zou, T., Jiang, D., 2016. “Influence of rising sea level on tidal dynamics in the Bohai Sea”. *J. Coast. Res.* **74**(sp1): 22–31.
[21] Fang, G., Wang, Y., Wei, Z., Choi, B.H., Wang, X., Wang, J., 2004. “Empirical cotidal charts of the Bohai, Yellow, and East China Seas from 10 years of TOPEX/Poseidon altimetry”. *J. Geophys. Res. Oceans* **109**(C11).
[22] Yao, Z., He, R., Bao, X., Wu, D., Song, J., 2012. “M2 tidal dynamics in Bohai and Yellow Seas: A hybrid data assimilative modelling study”. *Ocean Dyn.* **62**(5): 753–769.
[23] Teng, F., Fang, G.-H., Wei, Z.-X., Xu, X.-Q., Cui, X.-M., Wu, D., 2016. “Tidal simulation in Chezy-type and generalized Manning-type friction for Chinese Eastern Shelf Seas”. *Oceanol. Limnol. Sin.* **P731.23**.
[24] Adcock, T.A.A., 2015. “On tidal stream turbines placed off headlands”. *J. Renew. Sust. Energ.* **7**(6): 061706.
[25] Zhang, H., Li, Y., Zou, T., Tang, C., 2014. “Interaction between coastline change and tidal system of the Bohai Sea”. In: *2014 Ocean Sciences Meeting, Honolulu, HI, USA*.
[26] Chen, Y., Lin, B., Lin, J., Wang, S., 2017. “Experimental study of wake structure behind a horizontal axis tidal stream turbine”. *Appl. Energ.* **196**: 82–96.
[27] Blunden, L.S., Bahaj, A.S., 2006. “Initial evaluation of tidal stream energy resources at Portland Bill, UK”. *Renew. Energ.* **31**(2): 121–132.
[28] European Marine Energy Centre, 2009. “Assessment of Tidal Energy Resource”. Marine Renewable Energy Guides.
[29] Garrett, C., Cummins, P., 2008. “Limits to tidal current power”. *Renew. Energ.* **33**(11): 2485–2490.
[30] Vennell, R., Funke, S.W., Draper, S., Stevens, C., Divett, T., 2015. “Designing large arrays of tidal turbines: A synthesis and review”. *Renew. Sust. Energ. Rev.* **41**: 454–472.